## SEISMOLOGY

# The Khubsugul Earthquake of January 12, 2021, $M$w = 6.7, Northern Mongolia: Geological Effects and Tectonic Position of the Source

**A. N. Ovsyuchenko[a,b,]\*, S. Demberel[c], Y. V. Butanayev[c,d], N. G. Koshevoy[a,b],**
**Ts. Batsaikhan[c], and N. Baatar[d]**

Presented by Academician V.V. Yarmolyuk March 13, 2023

**Abstract**—The geological effects of the Khubsugul earthquake of January 12, 2021, with $M$w = 6.7, which became the strongest in the Khubsugul region during the instrumental stage of seismological observations, are studied and mapped. Using the ESI-2007 scale, the epicentral zone with intensity VIII is contoured. The primary seismic rupture is represented by the right-lateral strike–slip with a displacement amplitude up to 20 cm, which renewed the Late Holocene tectonic scarp on the western side of the Khubsugul rift basin. The dynamics of rupturing in the Late Holocene indicates the gradual expansion of the basin due to the destruction of the adjacent mountain range. The data of satellite interferometry and seismological observations are in good agreement with the results of the field studies, which allows considering the delineated region of maximum shaking as a projection of the upper part of the source zone onto the surface.

Seismicity is known to reflect the current tectonic processes in the Earth's subsurface. The geological manifestations of the earthquakes on the surface make it possible to obtain direct data on the macroseismic effect in the near zone, the spatial parameters of the seismic source, and the history of such events in the recent past [5]. The study of each recent strong earthquake according to a certain procedure yields new data on the structural patterns of the source zones and orientation of current geodynamic processes under conditions of a particular seismotectonic structure.

The Khubsugul earthquake of January 12, 2021, occurred on the southwestern flank of the Baikal rift system (BRS) and became the strongest event of the Khubsugul region during the instrumental period of observations (Fig. 1). For the BRS, there are well-developed geodynamic models. However, among the strongest earthquakes in the BRS studied representatively in terms of seismotectonics, for which seismotectonic manifestations on the surface were studied in detail and the ideas about the tectonic structure of the source were formed, we can mention only the 1950 Mondy earthquake with $M_s = 7$ [11] and the 1957 Muya earthquake with $M_s = 7.6$ [6]. Together with the 1967 Tas-Yuryakh earthquake ($M_s = 7$), these events became the strongest in the BRS during the instrumental period of observations. Thus, in terms of state of exploration of the seismotectonic conditions for strong earthquakes to occur in the BRS by direct methods, there is a certain deficit.

According to the data of the Altai-Sayan and Baikal branches of the Unified Geophysical Service, Russian Academy of Sciences, the Khubsugul earthquake had $M_w = 6.7$, $M_L = 6.9$, the focal depth was about 8 km, and the predicted intensity of shaking at the epicenter was $I_0 = 9$ [2]. The solutions of the focal mechanism obtained by the different authors differ slightly and indicate primarily fault kinematics of displacement in the source with a shear component [2, 8–10]. In general, this mechanism is typical of the BRS and reflects

*[a] Schmidt Institute of Physics of the Earth,*
*Russian Academy of Sciences, Moscow, 123995 Russia*
*[b] Geological Institute, Russian Academy of Sciences,*
*Moscow, 119017 Russia*
*[c] Institute of Astronomy and Geophysics,*
*Mongolian Academy of Sciences, Ulaanbaatar, Mongolia*
*[d] Tuva Institute for the Integrated Development of Natural*
*Resources, Siberian Branch, Russian Academy of Sciences,*
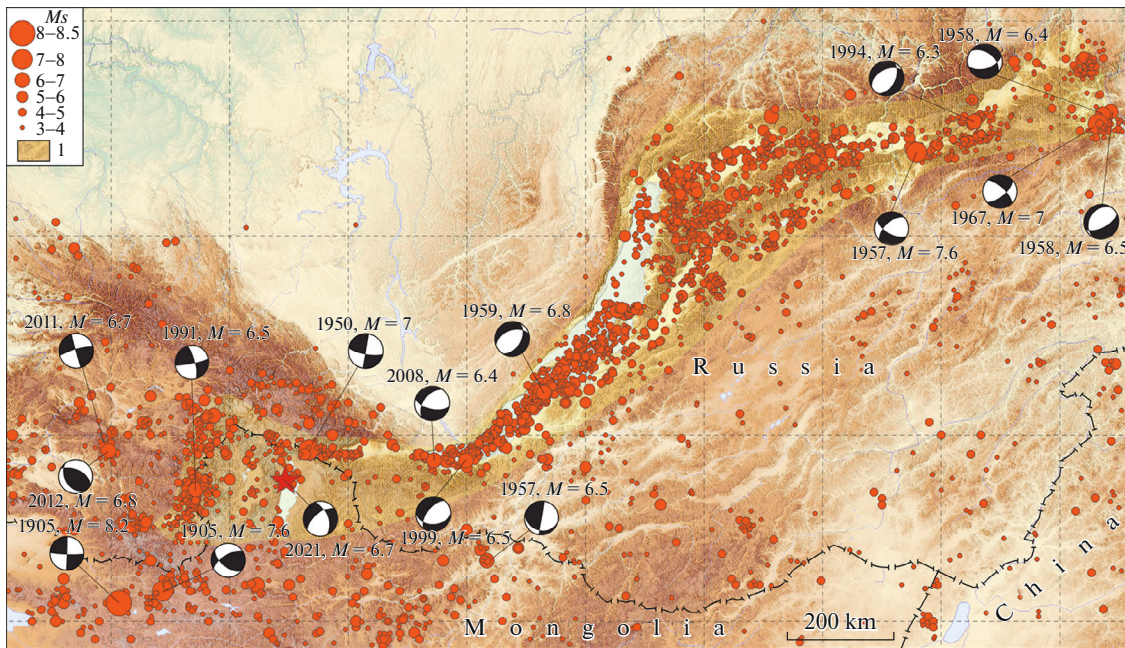*Kyzyl, 667007 Russia*
*\*e-mail: ovs@ifz.ru*

**Fig. 1.** Position of the epicenter of the 2021 Khubsugul earthquake (marked by the star) on the map of seismicity of the Baikal rift system and the adjacent territories. The earthquake epicenters since 1900 are indicated based on the data of the Earth's eigenoscillations GSR-2012 maps (www.seismorus.ru) and the Unified Geophysical Service, Russian Academy of Sciences (http://www.ceme.gsras.ru). For the strongest seismic events, the source mechanisms are presented according to the data in [3, 13]. The source mechanism of the 2021 Khubsugul earthquake is based on the data in [10]. (1) The Baikal rift system.
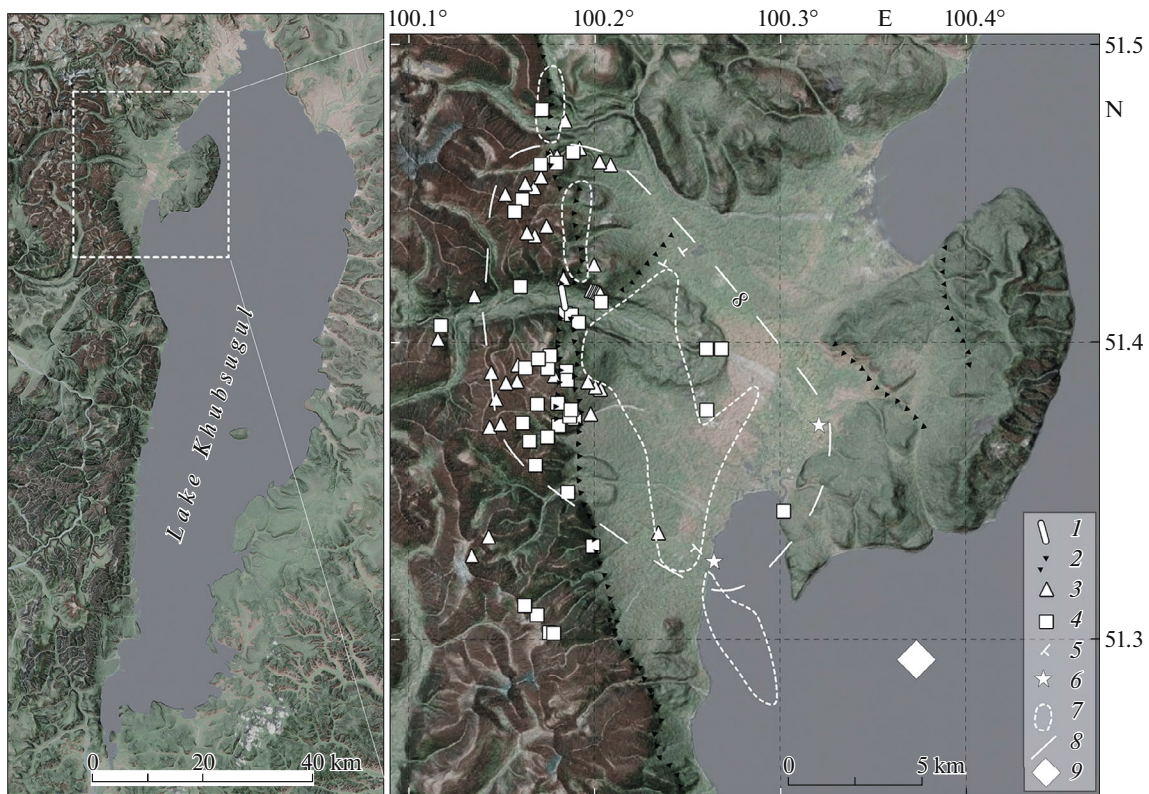


**Fig. 2.** Map of geological effects of the Khubsugul earthquake compared to the seismological data. (*1*) Seismic rupture; (*2*) tectonic scarps; (*3*) landslides; (*4*) rock falls; (*5*) seismo-gravitational fractures; (*6*) bursts of moist sand (dilutions); (*7*) maximum density of aftershocks (35−47 within the circle of 0.02° radius) according to the data in [2]; (*8*) isoseist VIII on the ESI-2007 scale (contour of the epicentral area); (*9*) earthquake epicenter according to the data in [2].

**Fig. 3.** Photo of secondary and primary effects of the Khubsugul earthquake. (a) Landslide. (b) A rock lump detached from the slope with an impact hollow. (c, d) Seismotectonic ruptures of shear kinematics.

a deformation regime of transtension (extension with shear).

Tectonically, the source is located on the western margin of the Khubsugul rift basin. The basin developed under conditions of extension and has the structure of an asymmetric semi-graben with a steep western and flat eastern margin [4]. The basin structure is dominated by active faults and submeridional strike–slip faults, confining the western margin of the basin. The shear component is oriented to the right along the NW-striking faults and to the left in the case of NE orientation [1]. The epicenter is located in the water area of Khubsugul Lake, which made it difficult to relate to a certain fault.

The primary geological survey of the epicentral area was performed three days after the earthquake by the specialists of Institute of Astronomy and Geophysics, Mongolian Academy of Sciences [8]. At that time, they recorded only secondary dislocations, such as seismo-vibrational fractures and bursts of moist sand on the plain of Khubsugul Lake.

In August 2022, we completed the field seismotectonic study of the earthquake source zone. The earthquake did not cause casualties or damage even in the epicentral zone. The mapped dislocations are clearly divided into two groups: primary ones reflecting earthquake source exposure on the surface as a seismotectonic rupture and secondary ones representing a result of seismic shaking (Fig. 2).

The distribution of secondary dislocations is determined by the geomorphological conditions and the distance to the source. They are represented by small landslides, slope detritus, rock falls, shaken slopes, seismo-gravitational fractures on the edges of the watershed slopes and terrace cusps,and seismo-vibrational fractures and bursts of moist sand on the surface of the swampy accumulative plain near Khubsugul Lake (Figs. 3a, 3b). To estimate the shaking intensity by the parameters of secondary dislocations, we used the ESI-2007 scale (Environmental Seismic Intensity), corresponding to the conventional scales of the MSK-64 and EMS-98 types [12], which we tested on several modern counterparts, including in the epicentral zone of the Tuva earthquakes of 2011–2012 [5]. Using the average sizes of seismo-vibrational fractures (25–40 m long at a width of up to 30 cm), the size of rock lumps detached from the slopes (up to $2.5 \times 3$ m $\times$ 25–30 m), and the landslide volume (20000–30000 $m^3$), we calculated intensity of VIII, which also corresponds to the parameters of seismotectonic dislocations. We contoured the epicentral zone based on these data.

At the place of dense secondary dislocations, we recorded thet surface exposure of the earthquake, which is a seismic rupture represented by the right-lateral strike–slip with displacement up to 20 cm in the vertical and horizontal planes (Figs. 3c, 3d). The rupture displaces all land forms on its way, shrubby-moss cover, stones, roots, and stems of the trees, which were
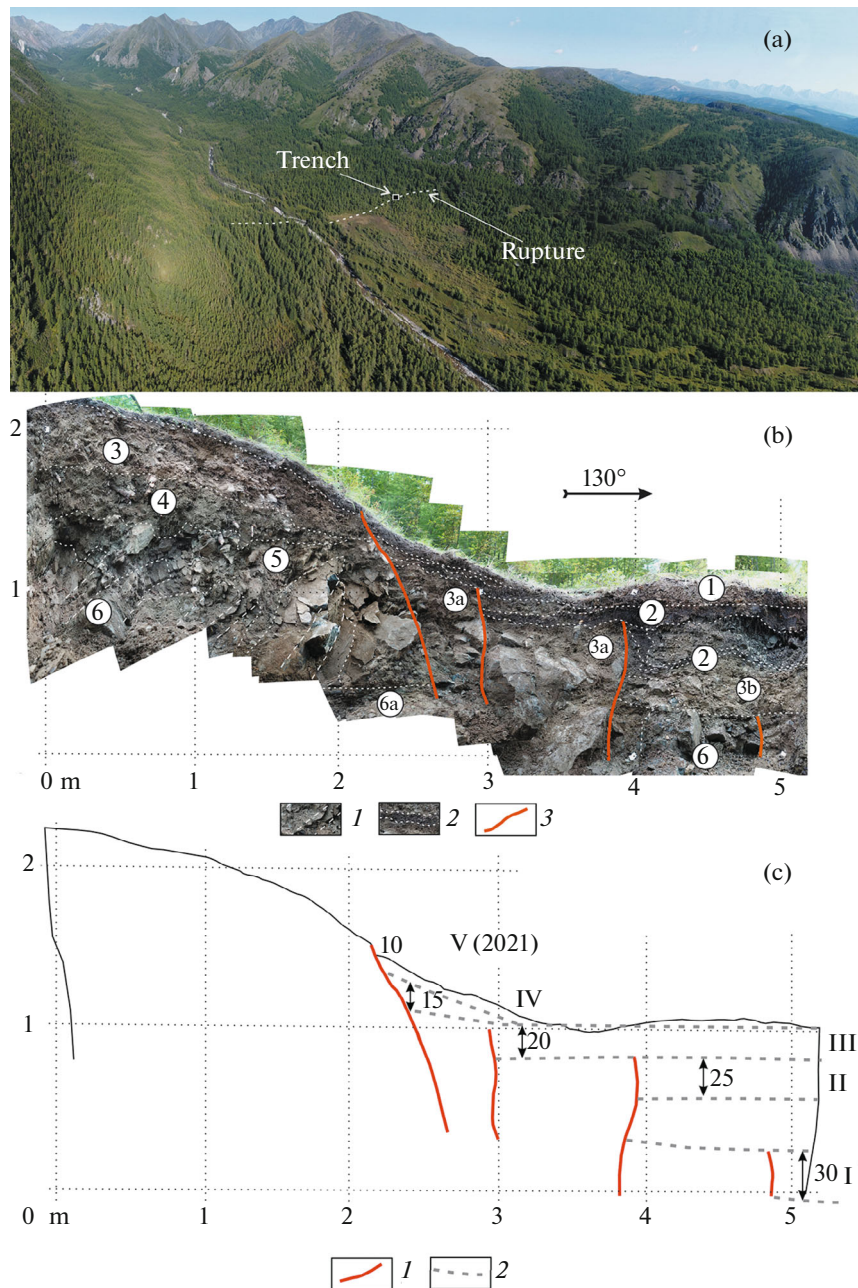
**Fig. 4.** Seismic rupture of the Khubsugul earthquake, position, and records of the trench. (a) Airphoto with the position of the mapped segment of the seismic rupture and the trench. (b) Panoramic photo of the northern wall and interpretation of the trench section. (*1*) Fracturing in bed rocks; (*2*) boundaries of the layers; (*3*) ruptures. Numbers in circles: (1) top soil; (2) peat; (3) loose, silty loams with debris, and scree (slope detritus), (3a) the same, with lumps of rock (colluvium), (3b) the same, compact, lumpy, gleic; (4) gray−green sand clays with scarce debris and scree (finely dispersed weathering crust); (5) debris, lumps with sandy-loam filler (debris weathering crust); (6) ultrabasic, intensely fractured bedrocks, (6a) the same, weathered to clay. (c) Reconstruction of the sequence of movements. (*1*) Ruptures; (*2*) position of the subsided fragments of the ancient surface of the Earth (numbers designate amplitudes of displacements, cm). Roman numerals number the sequence of seismotectonic displacements.

used to measure the displacement amplitude. The rupture is N-NW striking (340°−350°) and is recorded over about 250 m. The short length of the recorded rupture is likely determined by its weak significance and small displacement.

The tectonic nature of the rupture is highlighted by its confinedness to the tectonic scarp, which was formed by the previous motions. A trench was made ~1 m high across the strike of the scarp, which was renewed during the 2021 earthquake; the trench revealed the fault with a dip at an angle of 50°−70° eastward (Fig. 4). At the scarp edge, the rupture displaces the current surface of the Earth and the soil for 15−20 cm. At the base of the scarp, the ruptures of past earth-

quakes are exposed, which made new segments consistently subside from the side of the ridge. Thus, the rupture-formation dynamics in time and space indicates the expansion of the basin in the westerly direction with the subsequent capture and destruction of the adjacent mountain uplift.

The renewed tectonic scarp constitutes an en-echelon system of tectonic scarps mapped at the base of the ridge at the western limit of Khubsugul basin (Fig. 2). The scarps are Late Holocene, cut into the surfaces of moraines and river terraces in the river valleys, and form a chain of triangular tectonic facets between them.

According to the instrumental data, the earthquake epicenter is recorded 18−19 km southeast of the primary seismic rupture we discovered. It corresponds to the area of the maximum concentration of aftershocks [2]. The primary seismic rupture corresponds to the line with a sharp change in the interference image based on the data of satellite radar interferometry. The rupture model according to these data is represented by the NW-striking plane ($340°−350°$) with a dip angle of $45°−54°$ in the easterly direction, i.e., towards the hypocenter, reaching a depth of 18−24 km [7−10]. The maximum value of the displacement (1.2 m) on the basis of the modeling results is assumed at a depth of 7 km; subsidence of up to 20 cm is recorded on the surface [8, 10].

The data of modeling and seismological observations agree well with the results of field studies. The delineated area of maximum shaking corresponds to the area of maximum concentration of aftershocks based on the seismological data and is a projection of the upper part of the source onto the surface. The source subsides southeastward, i.e., towards the instrumental epicenter and the axial part of the Khubsugul basin at an angle of $50°−70°$ (Fig. 2). It has a regular morphostructural position and is confined to the active margin of the asymmetric Khubsugul rift basin, which is displaced towards the adjacent mountain group, making new segments consistently subside during each subsequent earthquake.

## FUNDING

## CONFLICT OF INTEREST

The authors declare that they have no conflicts of interest.

## OPEN ACCESS

## REFERENCES

1. A. V. Arzhannikova, A. V. Parfeevets, V. A. San'kov, and A. I. Miroshnichenko, Russ. Geol. Geophys. **44** (11), 1162−1167 (2003).

2. A. F. Emanov, A. A. Emanov, V. V. Chechel'nitskii, et al., Izv., Phys. Solid Earth **58** (1), 59−74 (2022).

3. L. P. Imaeva, V. S. Imaev, O. P. Smekalin, B. M. Koz'min, N. N. Grib, and A. V. Chipizubov, *Eastern Siberia: Seismotectonic Map* (Technical Institute (Branch) of M.K. Ammosov North-Eastern Federal Univ., Irkutsk-Neryungri, 2015) [in Russian].

4. V. M. Kochetkov, S. D. Khil'ko, Yu. A. Zorin, et al., in *Seismotectonics and Seismicity of the Cis-Khubsugul,* Ed. by V. P. Solonenko (Nauka, Novosibirsk, 1993) [in Russian].

5. E. A. Rogozhin, A. N. Ovsyuchenko, and A. S. Lar'kov, Geotectonics **55** (3), 307−334 (2021).

6. V. P. Solonenko, Izv. Akad. Nauk SSSR, Ser. Geol., No. 4, 58−70 (1965).

7. E. P. Timoshkina, V. O. Mikhailov, V. B. Smirnov, M. S. Volkova, and S. A. Khairetdinov, Izv., Phys. Solid Earth **58** (1), 74−80 (2022).

8. D. Battogtokh, A. Bayasgalan, K. Wang, D. Ganzorig, and J. Bayaraa, Mong. Geosci. **26** (52), 46−61 (2021).

9. Y. He, T. Wang, and L. Zhao, Remote Sens. **14**, 4553 (2022).

10. X. Liu, W. Xu, N. A. Radziminovich, N. Fang, and L. Xie, Tectonophysics **836**, 229407 (2022).

11. O. Lunina, A. Andreev, and A. Gladkov, J. Seismol., No. 19, 171−189 (2015).

12. A. M. Michetti, E. Esposito, L. Guerrieri, S. Porfido, L. Serva, R. Tatevossian, E. Vittori, F. Audemard, T. Azuma, J. Clague, V. Comerci A., Gurpinar, J. McCalpin, B. Mohammadioun, N. A. Morner, Y. Ota, and E. Rogozhin, Mem. Descritive Carta Geol. Ital. **74**, 41 (2007).

13. N. Radziminovich, G. Bayaraa, A. Miroshnichenko, S. Demberel, M. Ulziibat, D. Ganzorig, and A. Lukhnev, Geodynam. Tectonophys. **7** (1), 23−38 (2016).

*Translated by L. Mukhortova*

**Publisher's Note.** Pleiades Publishing remains neutral with regard to jurisdictional claims in published maps and institutional affiliations.